Heterogeneous Gas Chemistry in the CPFD Eulerian-Lagrangian Numerical Scheme (Ozone Decomposition)

Dale Snider, CPFD Software, 10899 Montgomery NE, LLC, Albuquerque, NM 87111
Sibashis Banerjee, Cristal Global, 6752 Baymeadow Drive, Gelne Burnie, MD 21060

Abstract

Heterogeneous catalytic chemistry is used throughout the chemical and petro-chemical industry. In predicting the performance of a reactor, knowing the gases and solids flow dynamics is as important as having a good chemical rate expressions. This paper gives the solution of ozone decomposition in a bubbling bed using the CPFD numerical scheme which is an Eulerian-Lagrangian solution method for fluid-solids flow. The ozone decomposition can be described by a single stoichiometric equation and has a first order reaction rate. The ozone decomposition is a standard problem for chemical analysis and has been used to characterize gas-solids contact in fluidized beds. The accuracy of predicting the ozone decomposition comes from correctly predicting the bed dynamics. The solution in this study is three-dimensional and predicts the coupled motion of both solids and gas. The chemical rate equation uses solids volume fraction, but the numerical method could calculate chemistry on the discrete catalyst, including a variation in size (surface area) if such a rate equation was available. The numerical results compare well with an analytic solution of the decomposition rate, and calculated results compare well with the experiment by Fryer and Potter (1976).

Introduction

Ozone decomposition is a standard problem for chemical analysis. It has been used to characterize the gas-solids contact in a fluidized bed. The ozone decomposition can be described by

$$2O_3 \rightarrow 3O_2 \tag{1}$$

and the ozone rate equation is

$$\frac{d[O_3]}{dt} = -c_s[O_3] \tag{2}$$

where [] denotes mole concentration. The rate coefficient is

$$c_s = k\,\theta_S \tag{3}$$

where θ_S is the solids volume fraction and k is a constant based on catalyst activity. The catalyst volume fraction in the chemical rate coefficient equation Eq. (3) does not account for the the effect of catalyst surface area (catalyst sites) from a particle size distribution (PSD). The solid-catalyst size distribution was not available, and a constant size was used in calculations.

The chemical process is simple, and at low concentration, the reaction is essentially irreversible and isothermal. Calculations were made for two stagnant beds and a fluidized bed. One static bed calculation is in a closed vessel where the ozone decomposition reaction increases the pressure. The second static bed calculation is in an open vessel which allows excess volume from the ozone decomposition to exit the vessel and leads to a decrease in mixture density. The ozone decomposition in the static beds has a known analytic decomposition rate and known pressurization in a closed vessel and known density in an open vessel. Because the full set of momentum and mass equations are solved, the static bed calculations provide a check on correctness of the predicted chemistry. The fluidized bed calculation is compared with measured data.

The calculations are made using the CPFD numerical scheme. The CPFD solves the fluid and

particle momentum, mass and energy. The particle momentum description is based on the multi-phase particle in cell (MP-PIC) method and the fluid phase is solution of the three dimensional Navier-Stokes equation. The calculations are made with the Barracuda™ software.

CPFD governing equations

The CPFD method solves the fluid and particle momentum equations in three dimensions The fluid is described by the Navier-Stokes equation with strong coupling with the discrete particles. The particle momentum follows the particle-in-cell (MP-PIC) numerical description from P. O'Rourke (Andrews, 1996; Snider, 1998; Snider, 2001) which is a Lagrangian description of particle motion described by ordinary differential equations with coupling with the fluid. The CPFD solution as applied in Arena-flow® and Barracuda-CPFD® is aimed at solving commercial problems, which are generally physically large systems. In the CPFD scheme, a numerical-particle is defined where particles are grouped with the same properties (species, size, density, etc.). The numerical-particle is a numerical approximation similar to the numerical control volume where a spatial region has a single property for the fluid. Using numerical particles, large commercial systems containing billions of particles can be analyzed using millions of numerical-particles.

The volume average two-phase incompressible continuity equation for the fluid with no interphase mass transfer is

$$\frac{\partial \theta_f}{\partial t} + \nabla \cdot \left(\theta_f \boldsymbol{u}_f \right) = 0 \,, \tag{4}$$

where $\mathbf{u}_f$ is the fluid velocity and θ_f is the fluid volume fraction. The volume average two-phase incompressible momentum equation for the fluid is

$$\frac{\partial \left(\theta_f \boldsymbol{u}_f \right)}{\partial t} + \nabla \cdot \left(\theta_f \boldsymbol{u}_f \boldsymbol{u}_f \right) = \frac{-1}{\rho_f} \nabla p - \frac{1}{\rho_f} \boldsymbol{F} + \theta_f \boldsymbol{g} + \frac{1}{\rho_f} \nabla \cdot \boldsymbol{\tau} \,, \tag{5}$$

where ρ_f is fluid density, p is fluid pressure, $\boldsymbol{\tau}$ is the macroscopic fluid stress tensor, and $\boldsymbol{g}$ is the gravitational acceleration. $\boldsymbol{F}$ is the rate of momentum exchange per volume between the fluid and particles phases. The fluid phase is compressible or incompressible (incompressible equations shown), and fluid and particle phases are isothermal.

The particle acceleration is

$$\frac{d \boldsymbol{u}}{dt} = D_p \left(\boldsymbol{u}_f - \boldsymbol{u}_p \right) - \frac{1}{\rho_p} \nabla p + \boldsymbol{g} - \frac{1}{\theta_p \rho_p} \nabla \tau_p \tag{6}$$

where $\boldsymbol{u}_p$ is the particle velocity, ρ_p is the particle density, $\boldsymbol{g}$ is gravity and τ_p is the particle normal stress. The terms represent acceleration due to aerodynamic drag, pressure gradient, gravity and gradient in the interparticle normal stress, τ_p.

Particle properties are mapped to and from the Eulerian grid. The interpolation operator is the product of interpolation operators in the three orthogonal directions. For a particle located at $\boldsymbol{x}_p$, where $\boldsymbol{x}_p=(x_p,y_p,z_p)$, the x-directional component of the interpolation operator to grid cell i, is an even function, independent of the y and z coordinates, and has the properties.

$$S_i^x(x_p) = \begin{array}{ll} 0 & x_{i-1} \geq x_p \geq x_{i+1} \\ 1 & x_p = x_i \end{array} \tag{7}$$

The x and y interpolation operators have a similar form. The particle volume fraction at cell ξ from mapping particle volume to the grid is

$$\theta_{p\xi}=\frac{1}{\Omega_\xi}\sum_{\iota}^{N_p}\Omega_p n_p S_{p\xi} \tag{8}$$

where Ω_ξ is a grid volume, Ω_p is particle volume, n_p is the number of particles in a numerical particle, and the summation is over all numerical particles N_p. From conservation of volume, the sum of fluid and particle volume fractions equals unity, $\theta_p+\theta_f=1$.

The implicit numerical integration of the particle velocity equation is

$$\boldsymbol{u}_p^{n+1}=\frac{\boldsymbol{u}_p^n+\Delta t\left[D_p\boldsymbol{u}_{f,p}^{n+1}-\frac{1}{\rho_p}\nabla p_p^{n+1}-\frac{1}{\rho_p\theta_p}\nabla\tau_p^{n+1}+\boldsymbol{g}\right]}{1+\Delta t\,D_p} \tag{9}$$

where $\boldsymbol{u}_{f,p}^{n+1}$ is the interpolated fluid velocity at the particle location, ∇p_p^{n+1} is the interpolated pressure gradient at the particle location, $\nabla\tau_p^{n+1}$ is the interpolated particle stress gradient at the particle location, D_p is the drag coefficient at a particle location. Particles are grouped into numerical-particles each containing n_p particles with identical properties located at position, $\boldsymbol{x}_p$. The numerical new-time particle location is

$$\boldsymbol{x}_p^{n+1}=\boldsymbol{x}_p^n+\Delta t\,\boldsymbol{u}_p^{n+1} \tag{10}$$

The interphase drag coefficient is

$$D_p=C_d\frac{3}{8}\frac{\rho_g}{\rho_p}\frac{\left|\mathbf{u}_f-\mathbf{u}_p\right|}{r}, \tag{11}$$

and the Wun and Yu (1966)drag correlation is used

$$\begin{aligned}&\mathrm{Re}<1000 \quad C_d=\frac{24}{\mathrm{Re}}\left(1+0.15\,\mathrm{Re}^{0.687}\right)\theta_f^{-2.65}\\&\mathrm{Re}\geq 1000 \quad C_d=0.44\,\theta_f^{-2.65}\end{aligned} \tag{12}$$

$$\mathrm{Re}=\frac{2\rho_f\left|\boldsymbol{u}_f-\boldsymbol{u}_p\right|r}{\mu_f}\quad, \tag{13}$$

where μ_f is the gas viscosity and the particle radius is

$$r=\left(\frac{3\Omega_p}{4\pi}\right)^{1/3} \tag{14}$$

Particle-to-particle collisions are modeled by the particle normal stress. The particle stress is derived from the particle volume fraction which is in turn calculated from particle volume mapped to the grid. The particle normal stress model used here is (Snider, 2001)

$$\tau=\frac{P_s\theta_p^\beta}{max\left[\left(\theta_{CP}-\theta_p\right),\epsilon\left(1-\theta_p\right)\right]}\quad, \tag{15}$$

where ε is a small number on the order of 10^{-7} to remove the singularity. The close-pack limit is somewhat

arbitrary and depends on the size, shape and ordering of the particles. Therefore the solution method allows the particle volume fraction, at times, to slightly exceed close-pack which is physically possible considering that shifting or rearranging of granular materials may occur. The particle normal stress is mapped and applied to discrete particles. Because particles have subgrid (no grid) behavior, the application of the normal stress gradient to a discrete particle is modeled and accounts for the particle properties and whether the particle is moving with or against the stress gradient (Snider, 2001).

The conservation equations are approximated and solved by finite volumes with staggered scalar and momentum nodes. The fluid momentum equation implicitly couples fluids and particles through the interphase momentum transfer. The interphase momentum transfer at momentum cell ξ is

$$F_{\xi}^{n+1}=\frac{1}{\Omega_{\xi}}\sum_{p} S_{\xi}\left[D_p\left(\boldsymbol{u}_{f,p}^{n+1}-\boldsymbol{u}_{p}^{n+1}\right)-\frac{1}{\rho_p}\nabla p_p^{n+1}\right] n_p m_p \quad , \tag{16}$$

Particle drag and properties are interpolated to the grid. If a top hat interpolation is used, the fluid velocity at particle position $\boldsymbol{x}_p$ is either zero or the node velocity. If a trilinear or other interpolation is used, the fluid velocity at particle position $\boldsymbol{x}_p$ includes the node velocities in support of the interpolation.

Mass continuity is from the material motion of particles. The mixture fluid mass is calculated from volume continuity, $\theta_f=1-\theta_p$ A SIMPLE solution scheme with a coupled solids momentum is used to adjust pressure, density and fluid velocity to satisfy fluid continuity. Velocity, pressure and density correction dependence, estimated from the momentum equation are entered into the fluid continuity equation, giving a semi-implicit coupling of mass and momentum in a pressure correction equation. The pressure equation is solved and fluid pressure, density and velocities are corrected to satisfy continuity.

The gas mixture properties are from the mass fractions of the individual gas species properties. An ideal gas equation of state is used for the pressure-density dependency. Gas species transport is calculated from the bulk mixture flow. The Livermore National Laboratory CVODE ordinary differential equation (ODE) solver (Hindermarsh and Serban, 2006), is used to calculate the chemistry rate. For the simple ozone decomposition in this work, the CVODE solver , which is for sparse/stiff ODE equation sets, is over-kill.

Analytic solution for uniform packed bed

If a fluidized bed has an ideal uniform solid distribution, there is an analytic solution for the decomposition of ozone. The one dimensional transport of ozone through a bed is described by

$$\rho_{mix}\theta_f u\frac{dY_{O_3}}{dz}=\theta_f\rho_{mix}\frac{dY_{O3}}{dt} \tag{17}$$

where ρ_{mix} is the gas mixture density, u is the fluid velocity, z is the axial distance, Y_{O3} is the mass fraction of O_3 and θ_f is the fluid volume fraction. The first order reaction, given by Eq. (2), is substituted into Eq. (17) giving the rate of production of ozone

$$\rho_{mix}u\frac{dY_{O_3}}{dz}=-\rho_{mix}k\theta_p Y_{O_3} \tag{18}$$

The mass fraction is

$$Y_{O_3}=Y_{O_3}^{o}e^{-\frac{k\theta_p}{u}z} \tag{19}$$

where Y^o is the initial value (at t=0). The superficial velocity is $U=\theta_f u$, which is substituted into Eq (18)

giving

$$Y_{O_3} = Y^o_{O_3} e^{-\frac{k\theta_p\theta_f}{U}z} \tag{20}$$

Figure 3 shows that the Barracuda calculation for a uniform bed of solids compares well to the analytic solution Eq. (20). Because the gas velocity was well above the minimum fluidization velocity, the ideal bed would not be stationary and therefore, the solids were forced to be stationary. While this is not physically correct for solid dynamics, it gives a constant uniform distribution of solids from which the chemistry could be tested.

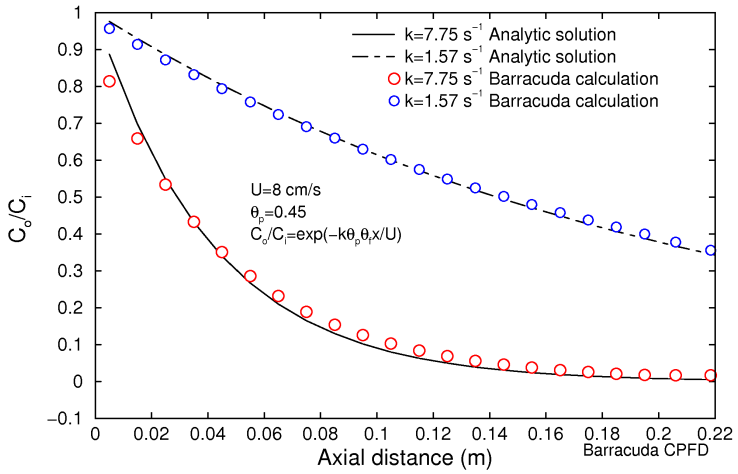

Figure 1. Barracuda calculation compared with analytic solution.
Analytic solution uses k=1.57 s^{-1} and k=7.75 s^{-1}, θ_p=0.45, and x=11.5 cm.

Fluidized bed ozone decomposition

The ozone decomposition is calculated in a fluidized bed. The experiment by Fryer and Potter (1976) is modeled. The experiment vessel was 22.9 cm diameter and 200 cm tall. The packed bed contains solid catalyst of silica sand impregnated with Fe_2O_3 .The bed is fluidized with dry air with O_3 added. The parameters are listed in Table 2. All calculations were run for the full three-dimensional bed.

Figure 2 shows the solids in the fluidized bed colored by volume fraction. The volume fraction spatial parameter is mapped to the discrete particle locations for visualization. The bed is bubbling, and like the experiment, the inner details of the bed are not distinct. Figure 3 shows the solid volume fraction by two other graphic methods in a cut section of the bed. Figure 3a shows the volume fraction of solids on the Eulerian grid, which is similar to calculated data using an Eulerian representation of solids. The light areas are void structures or "bubbles", and the dark areas are more dense packed regions of solids. Figure 3b shows the solid volume fraction greater than 0.3. The holes are the void structures of gas rising through the bed.

Figure 4 shows the mass fraction of O_3 next to the solids in the fluidized bed. The view is with the front half of the bed removed. The ozone enters the bed at 0.1 mass fraction and starts decomposing to oxygen in the presence of the catalyst. At the bottom of the bed, the catalyst is relatively uniformly mixed compared to higher in the bed where multiple "bubbles" have formed. This uniform catalyst-gas mixture gives a near uniform O_3 decomposition for the first few centimeters. Further up in the bed, plumes of O_3 rise in the bed in gas voids ("bubbles") while O_3 in denser packed regions of catalyst decompose to oxygen. Above the bed, O_3 which did not decompose to O_2 drifts in the bulk flow and flows out of the bed.

The prediction of the ozone decomposition in a fluidized bed requires accurate prediction of the bed dynamics. In calculating fluidized beds, it is common to adjust the drag coefficient based on a measured fluidization velocity. This allows calculations which use a single particle size to adjust to a best-fit particle size for the calculation. This adjustment also allows a correlation to better represent a particular system. In this study, there were no adjustments in calculation parameters to fit or tune the calculation for the problem. The performance of the drag model is deduced from the predicted pressure, as the inlet velocity is ramped with time. Fryer and Potter (1976) reported the measured minimum fluidization velocity (U_{mf}) was 1.7 cm/s and Fig. 5 shows from the calculated U_{mf} is approximately 1.6 cm/s. A solid size distribution was not available for this study, and possible inaccuracies in calculation parameters with respect to experimental conditions, including inaccuracy in the drag correlation are possible sources for the small discrepancy between measured and calculated U_{mf}. From the relatively good comparison between measured and calculated minimum fluidization velocity, the standard Win and Yu (1966) is judged sufficient without adjustment.

Table 2. Simulation conditions for a fluidized bed

Vessel diameter	22.9 cm
Vessel height	30 cm
Top pressure boundary for open vessel	101 kPa
Temperature	300 K
Inlet mixture N_2	0.702 mass fraction
Inlet mixture O_2	0.198 mass fraction
Inlet mixture O_3	0.1 mass fraction
Mixture flow rate	ranges from 2 to14 cm/s
Solid-catalyst	Fe_2O_3 with a silica base
Solid-catalyst density	2655 kg/m^3
Solid-catalyst radius	60 μm [1]
Solid-catalyst sphericity	1
Reaction rate constant, k	0.33 to 1.57 s^{-1} [2]
Initial solid-catalyst volume fraction	0.6

1. No information was given on the particle size distribution
2. Units from reaction rate equation, (s^{-1}).

The fluidized bed calculations were run sufficiently long at a fixed inlet flow rate to get a quasi steady rate of ozone decomposition. Figure 6 shows the ozone at the top of the vessel for an inlet flow rate of 7 cm/s and a chemical rate coefficient k= 1.57 s$^{-1.}$ At 24 s, the inlet velocity is increased to 11 cm/s and the calculation continues to run beyond the time period shown in the figure. Figure 7 shows the calculated and measured ozone decomposition as a function of inlet flow rate. The comparison is excellent. As the inlet flow rate increases, less ozone decomposes to oxygen. In the bubbling fluidized bed, ozone moving in bubbles bypasses solid catalyst contact. The prediction from the analytic solution for a uniform, stationary packed bed also compares well with the measured ozone decomposition. This is partly due to choosing the solids volume fraction for the analytic solution from the CPFD calculation. In general, an a priori effective solids volume fraction can not be chosen for a fluidized bed.

Figures 8 and 9 show the calculated ozone decomposition for k=0886 s^{-1} and k=0.33 s^{-1}, respectively. The comparison between Barracuda and experiment is also good. The calculation is shifted a little above or a little below the measured decomposition data. The variation could be from slightly different calculation parameters from those used in the experiments. There was a range of measured rate coefficients that where combined to get the average coefficient which is used in the Barracuda calculation. For the average k=7.75, Fryer and Potter reported rate constants from 7.05 to 8.05. The reaction rate from

this range of measured coefficients can produce a variation in decomposition of ozone from -105% to 26% relative to the average reaction constant (analysis based on analytic solution). The ozone enters the bed at 1.5 cm from the bottom, while Barracuda calculations have ozone entering at the bottom. As noted by Fryer and Potter (1976) this gives an effectively shorter ozone decomposition zone. A 11.5 cm deep bed has a 13% smaller effective reaction zone. For a 24 cm deep bed, the effective reaction zone is 6% smaller. Again, the the analytic solution for a uniform packed bed compares well with the measured data.

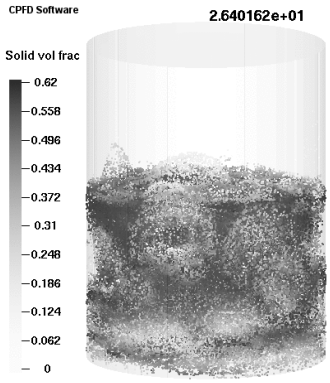

Figure 2. Calculated solids distribution. Discrete solids are shown colored by volume fraction mapped from the grid to particle locations.

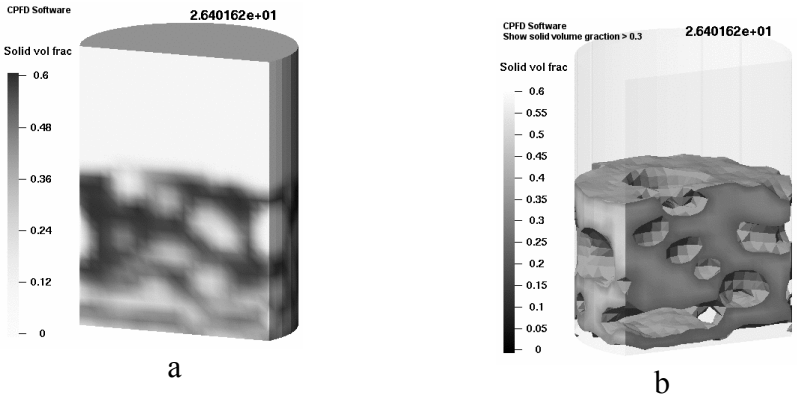

Figure 3. Calculated solids field, colored by volume fraction. U_{inlet}=11 cm/s, static bed height is 11.5 cm and k=1.57 s^{-1}. Figure b shows volume fraction greater than 0.3.

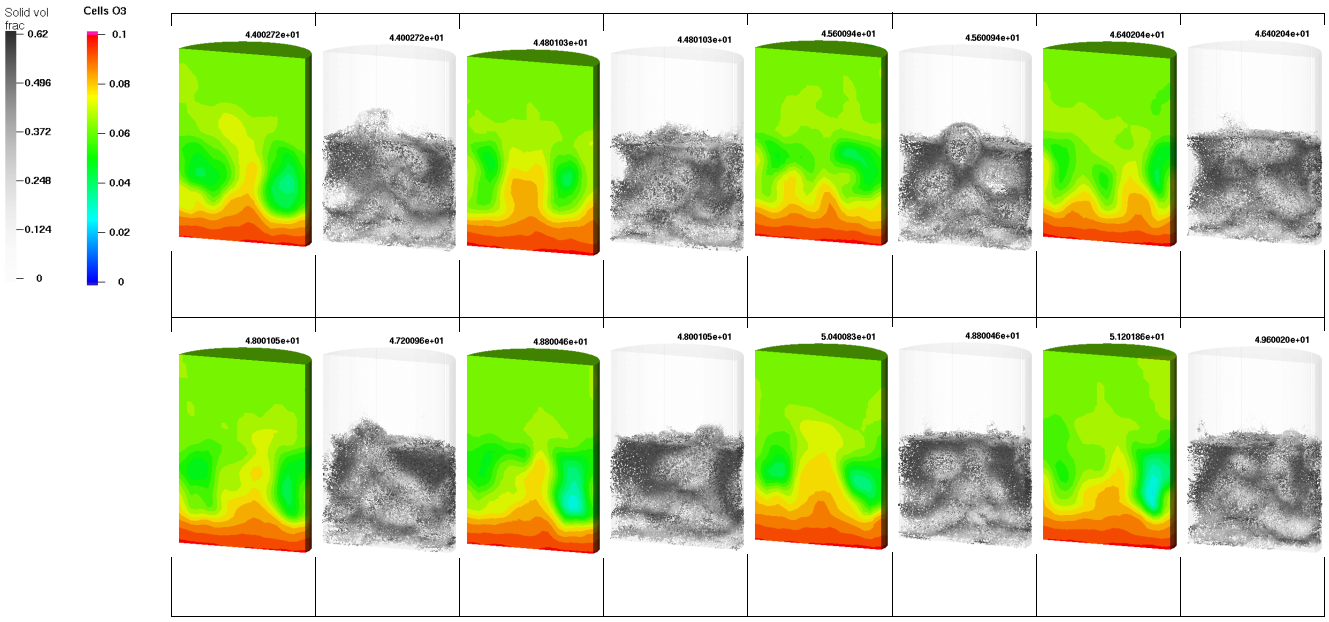

Figure 4. Calculated O_3 mass fraction and catalyst-solids colored by volume fraction. U_{inlet}=11 cm/s, static bed height is 11.5 cm and k=1.57 s^{-1}.

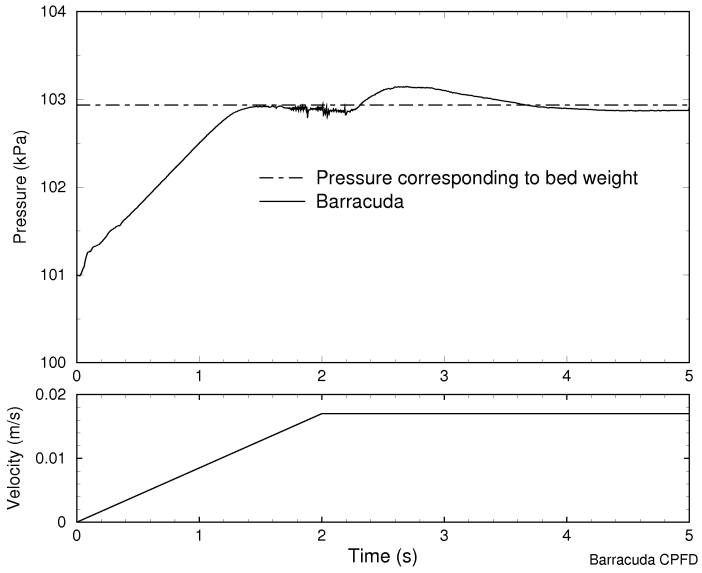

Figure 5. Calculated transient pressure and inlet gas-mixture velocity leading to minimum fluidization. Static bed height of 11.5 cm and reaction rate coefficient k=1.57 s^{-1}

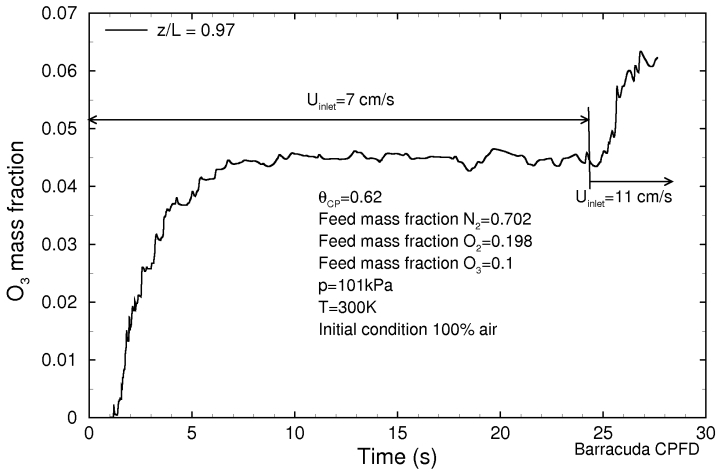

Figure 6. Calculated transient O_3 mass fraction at inlet mixture velocity of 7 cm/s, static bed height of 11.5 cm and reaction rate coefficient k=1.57 s^{-1}

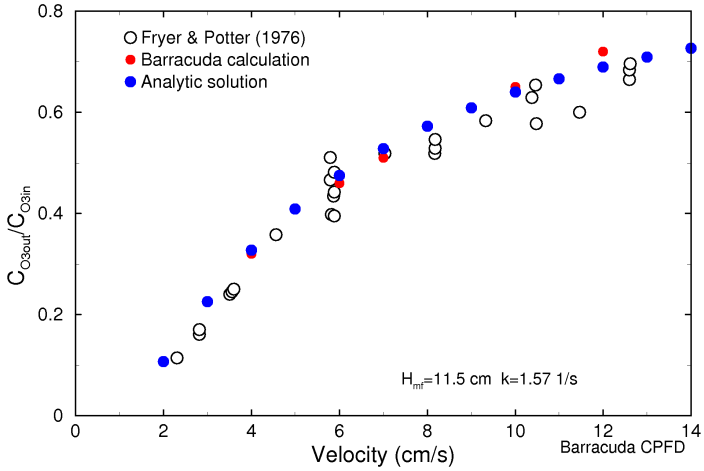

Figure 7. Measured and calculated O_3 normalized mass fraction as function of inlet velocity. Static bed height is 11.5 cm and chemical rate constant 1.57 s^{-1}. Analytic solution uses k=1.57 s^{-1}, ρ_f=1.2 kg/m^3 θ_p=0.45, and x=11.5 cm.

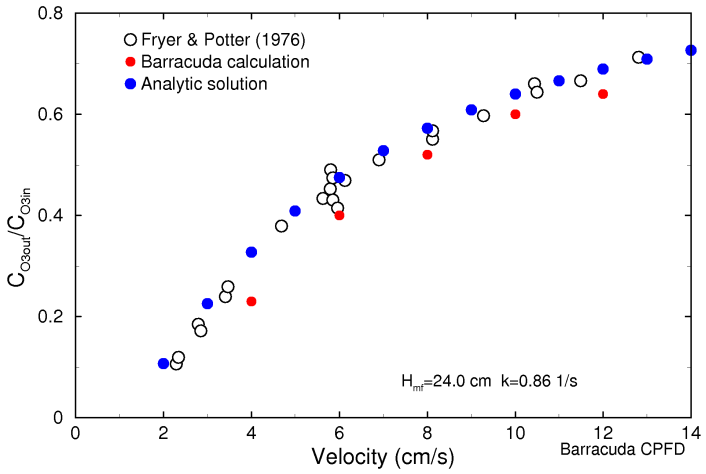

Figure 8. Measured and calculated O_3 normalized mass fraction as function of inlet velocity. Static bed height is 24 cm and chemical rate constant 0.86 s^{-1}. Analytic solution uses k=0.86 s^{-1}, ρ_f=1.2 kg/m^3 θ_p=0.45, and x=24 cm.

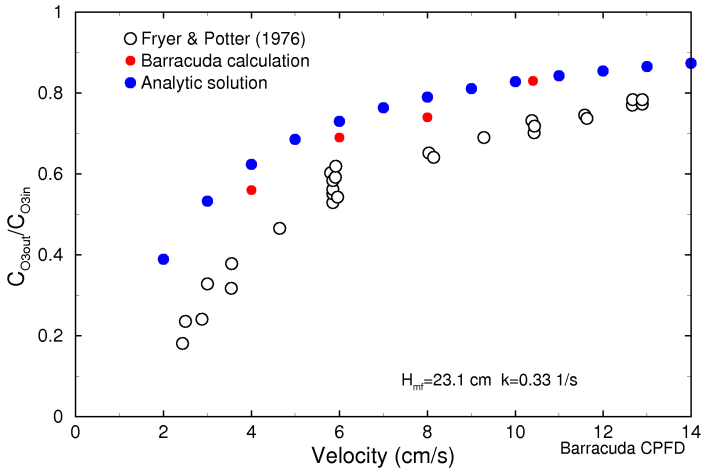

Figure 9. Measured and calculated O_3 normalized mass fraction as function of inlet velocity. Static bed height is 23.1 cm and chemical rate constant 0.33 s^{-1}. Analytic solution uses k=0.33 s^{-1}, ρ_f=1.2 kg/m^3 θ_p=0.45, and x=23.1 cm.

Concluding remarks

The implicit solution of the ozone decomposition and explicit calculation of oxygen generation was calculated well by the CPFD numerical method. The fluidized bed calculation predicted the "usual" void structures or "bubbles"; however, there were instantaneous complex solids and gas flow patterns. The ozone chemistry is a simple and well behaved reaction rate. The correct calculation of the chemistry depends on correct calculation of the bed motion. The bubbles transport gas with little gas-catalyst contact which reduces the chemistry yield. In this study, the complete set of fluid and solid mass and momentum equations, and the chemistry equations were solved. All calculations were made in three dimensions, and no parameters were tuned or adjusted to fit the experiment.

The analytic ozone decomposition solution also compared well to the experimental data. The good agreement is not surprising considering that the catalyst concentration in the analytic solution was from the CPFD bubbling bed calculation. In general, the bed dynamics and solids concentration are unknown, and if the bed has streamers or various degrees of mixing, a suitable average solids concentration cannot be simply chosen.

Reference

Andrews, M. J., and O'Rourke, P. J. (1996) The Multiphase Particle-in-Cell Method (MP-PIC) Method for Dense Particle Flow, Int. J. Multiphase Flow, 22, 379-402 .

Fryer, C. and Potter, O.E, (1976), "Experimental investigation of models for fluidized bed catalytic reactors," AIChE J., **22**.

Hindermarsh, A. C., and Serban, R., (2006), *User documentation for CVODE v2.5.0*, Center for Applied Scientific Computing, Lawrence Livermore National Laboratory, UCRL-SM-208108.

Snider, D. M., et al. (1998), Sediment Flow in Inclined Vessels Calculated Using Multiphase Particle-in-Cell Model for Dense Particle Flows, Int. J. Multiphase Flow, 24, 1359-1382.

Snider, D. M. (2001) An Incompressible Three-Dimensional Multiphase Particle-in-Cell Model for Dense Particle Flows," J. Comput. Phys*.,* 170, 523-549

Wen, C.Y. and Yu, Y.H., (1966) "Mechanics of fluidization," Chem. Eng. Progr. Symp., Ser. 62, 100-110.